



Calculation of numerical density of enamel prisms in multituberculate enamels: A review

GISLE FOSSE

In this brief review I explain the method of quantitatively describing prismatic enamel microstructure in multituberculates, to facilitate its practical use by paleontologists. I argue that histogenesis of gigantoprismatic enamel in many multituberculate taxa must have been quite exceptional in mammals. Future studies of enamel in plesiomorphic “plagiaulacidan” multituberculates are necessary to elucidate the evolutionary phases of enamel micromorphology toward prismatic mammalian enamel generally, and perhaps as a consequence, the origin of the successful (Late Cretaceous–Eocene) multituberculate suborder Cimolodonta and relationships among its subgroups. Such studies should therefore include calculation of numerical prism densities whenever possible.

Introduction

The enamels of advanced cimolodontan multituberculate teeth from the Paleocene Bug Creek Anthills locality in Montana were found to be prismatic (Fosse et al. 1973). It was later hypothesized that members of the suborder Taeniolabidoidea (*sensu* Sloan and Van Valen 1965)¹ had enamel with exceptionally widely spaced prisms never seen before in fossil or extant mammalian enamels, whereas members of the suborder Ptilodontoidea had enamels consisting of small prisms like all other known extinct or extant mammalian enamels. The exceptional taeniolabidoid enamel was called “gigantoprismatic” (Fosse et al. 1978). This hypothesis was confirmed independently seven years later by one North American team (Carlson and Krause 1985; Krause and Carlson 1986, 1987) and one European team (Fosse et al. 1985).

Institutional abbreviations.—DORCM, Dorset County Museum, Dorset, England; MNH, Museum of Natural History, London, England; PMO, Paleontological Museum, University of Oslo, Oslo, Norway; SPT, Institute of Speleology, Bucharest, Romania; ZPAL Institute of Paleobiology, Polish Academy of Sciences, Warsaw, Poland.

¹ Sloan and Van Valen (1965) divided advanced multituberculates (later Cimolodonta of McKenna 1975) into the suborders Taeniolabidoidea and Ptilodontoidea. Kielan-Jaworowska and Hurum (2001) gave superfamily rank to Taeniolabidoidea and Ptilodontoidea, and restricted Taeniolabidoidea to the single family Taeniolabididae (see also Fox 1999). The gigantoprismatic enamel recognized by Fosse et al. (1978) as characteristic of Taeniolabidoidea *sensu* Sloan and Van Valen (1965) is now known to also occur in two genera of the paraphyletic suborder ‘Plagiaulacida’, the informally-recognized *Paracimexomys* group, the superfamily Djadochtherioidea, five families *incertae sedis*, and some *incertae sedis* genera. The “normal” enamel (sometimes called micropismatic) always seen in extant mammals, occurs only in the superfamily Ptilodontoidea (see Kielan-Jaworowska and Hurum 2001 for details). As my paper is not systematic, but mainly technical, for simplicity I use the terms “suborder Taeniolabidoidea” and “suborder Ptilodontoidea” *sensu* Sloan and Van Valen (1965).

Numerical density of enamel prisms

In enamel formation of extant mammals, the closely apposed columnar ameloblasts are hexagonally arranged in cross sections planoparallel with the ameloblast/enamel contact surface. Each ameloblast produces one prism rod and half the thickness of its surrounding interprismatic enamel. Therefore the prisms are also hexagonally distributed in such sectional planes. The enamel prisms run from the dentin-enamel junction to the outer surface of the enamel mantle (Fosse 1968a, b). Hunter-Schreger bands seen in longitudinal sections characterize their centrifugal course in most mammalian enamels (Koenigswald and Sander 1997). Fig. 1 is a diagrammatic description of prismatic enamel in a section tangential to the enamel surface. The prisms are represented by hexagonally distributed circles. The hexagon in the lower left corner represents the cross sectional secretory area of one ameloblast producing a prism and half the thickness of interprismatic enamel along its peripheral rim. It is evident that there are as many contiguous hexagons with common sides as circles in the diagram. Such hexagons cannot easily be delineated and measured in a less regular prism pattern. However, the area of a tetragon with its corners in the centers of four adjacent cross-cut prisms equals the secretory area of one ameloblast, since there are as many contiguous tetragons as prisms in such a distributional pattern (Fosse 1968a). It is not difficult to plot approximate geometrical centers of cross-cut prisms. The area of each tetragon is the sum of the areas of the two triangles formed by the shorter diagonal. The area of a tetragon is thus easily calculated. One mm² divided by the mean tetragon area expresses the number of prisms per mm² and thus also the original ameloblast number per mm² (Fosse 1968b). The diameters of the prisms are without consequence for these values. Prismatic diameters vary independently from central distances between prisms, and only reflect diameters of Tome’s processes in ameloblasts (Fosse 1968a; Carlson and Krause 1985; Koenigswald and Sander 1997).

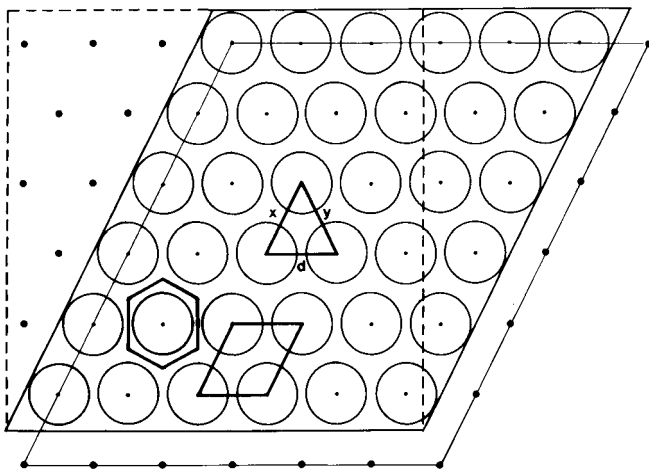


Fig. 1. Graphical description of cross sectioned, closely and regularly packed prisms in a slightly vertically distended hexagonal pattern. The hexagon in the lower left corner represents the secretory area of one ameloblast. Areas of hexagon and tetragon are equal, both expressing the size of the secretory area of one ameloblast. A triangle with corners in the centers of 3 adjacent prisms is the smallest unit for quantitative description of prism distribution and thus size and distribution of ameloblasts (from Fosse 1968a, b).

In Fig. 2, showing planed and etched enamel of the cimolodontan multituberculate *Meniscoessus* sp., the scale bar in the original photo represents 10 μm and measured 40 mm. The linear magnification was thus 4000x. The mean length of the sides of the traced pair of adjoining triangles constituting the tetragon in the original photo was 61.5 mm. The following proportion is then valid:

$$10/40 = d/61.5.$$

$$\text{Thus } d = (10 * 61.5)/40 = 15.375 \mu\text{m},$$

d being the true length of the mean triangle side, hence called central distance (CD), in the *Meniscoessus* enamel in Fig. 2. The number of cross-cut prisms per mm^2 is given by the general equation:

$$a = (2 * 10^6) / (d^2 * 3^{1/2})$$

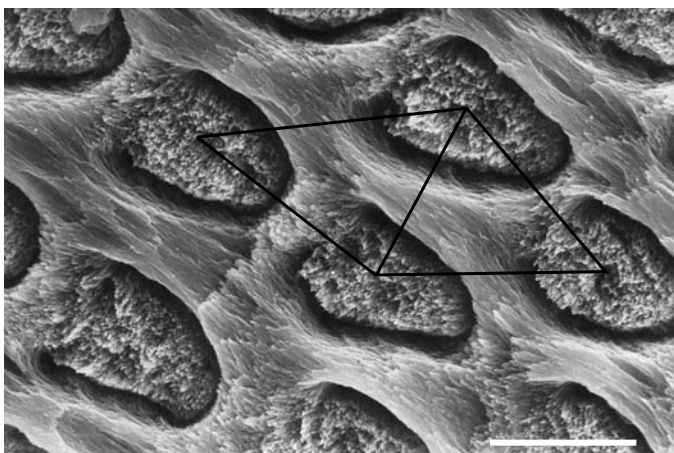


Fig. 2. SEM micrograph of gigantoprismatic enamel in m2 of *Meniscoessus* sp. ZPAL MK-I/9 (from Fosse et al. 1985). Traced tetragon visualizes size of original ameloblast secretory area. Either of its two triangles describes prism distribution. Regularly spaced prisms, numerical density 4884/ mm^2 , mean CD = 15.37 μm . Scale bar 10 μm .

where a is the number of prisms per mm^2 . The exponent “1/2” signifies square root. For the *Meniscoessus* specimen the numerical prism density in the micrographed enamel location is 4884/ mm^2 .

For any enamel the calculated mean CD and number of prisms/ mm^2 are never exact values but good statistical approximations. Only in small enamel areas are cross cut prisms regularly arranged as in Fig. 2. The numerical prism density is ideally computed by the mean tetragon area defined by the sides in a pair of triangles joined by one common side (Fosse 1968a). However, the average CD is less time consuming to calculate and use; this method was first applied by Carlson and Krause (1985). The results are close to and do not seem to deviate systematically from the density calculated by the mean tetragon area expressed by the contiguous triangles of the measured enamel surface.

When only four given cross cut adjacent prisms, describing one tetragon, are used for calculation, the errors in plotting centers and measuring the central distances will be greater than if several contiguous tetragons are traced (Fosse 1968a).

Except the untreated *Bolodon crassidens* enamel in Fig. 6, the following enamel micrographs depict planed and etched surfaces planoparallel with the natural outer enamel surface and have been presented in separate earlier publications by the author.

Gigantoprismatic enamels have until now been observed in numerous multituberculates (see footnote on p. 657 and Kielan-Jaworowska and Hurum 2001). In the superfamily Ptilodontoidea normal prismatic enamels seem characteristic, as well as in many other known extant and extinct mammals (Carlson and Krause 1985; Fosse et al. 1985; Krause and Carlson 1986, 1987). Central distances in gigantoprismatic enamel imply ameloblast diameters that have never been seen in any extant vertebrate. Moreover, to my knowledge no other secretory columnar epithelium with such large cells is known elsewhere in the body of extant mammals. Therefore it is safe to maintain that the gigantoprismatic enamel demonstrates a unique anatomical character in mammalian evolution.

The montage in Fig. 3 demonstrates the difference between gigantoprismatic and normal prismatic enamel. The magnification is the same in A and B, and in both micrographs the centers of 12 adjacent prisms have been connected in groups, each forming a continuous cluster of 12 triangles. The difference in size is obvious, but less striking than in many other comparisons between normal and gigantoprismatic enamels with identical magnification. Clusters of triangles describe more accurately the mean CD, the marginal errors in plotting and measuring single, separate triangles being reduced significantly. The drawn triangle clusters in A and B need not necessarily be identical with those used by calculation in the original micrographs.

Fig. 4 graphically demonstrates qualitatively the probability that gigantoprismatic enamels form their own morphological “class” or universe. To firmly support this supposition statistically, each single value should have been qualified by its standard deviation. To obtain this, deeper planing and thus more destructive methods would have been necessary. However, the variation in mean numerical prism densities did not seem significantly different in the two enamel types.

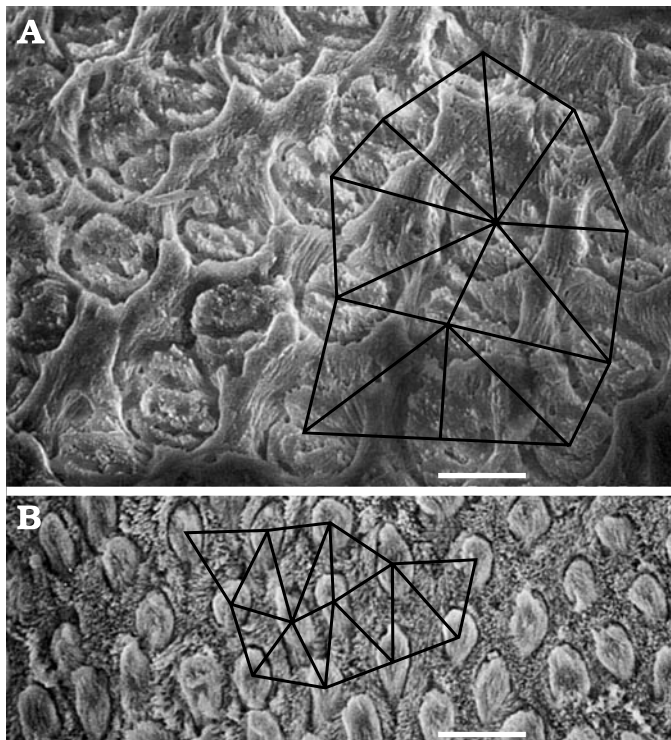


Fig. 3. Montage of SEM micrographs of gigantoprismatic and normal prismatic enamels (from Fosse et al. 2001). In this case the standard deviation of measured CD's was calculated. **A.** Gigantoprismatic enamel in P2 of *Kogaionon unguereanui*, SPT 001, with prismatic density of 5024/mm² and mean CD = 15.16 μ m (\pm 3.1). *Kogaionon* shows similarity to the Taenio-labididae in other respects also. **B.** Normal prismatic enamel in P4 of *Mesodma* sp., PMO 169.283, belonging to the superfamily Ptilodontoidea, with prismatic density of 21491/mm² and mean CD = 7.33 μ m (\pm 1.39). Scale bars 10 μ m.

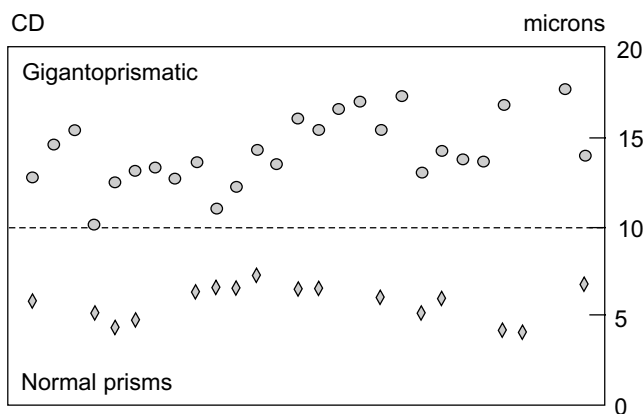


Fig. 4. Graph showing distribution of mean CDs in gigantoprismatic enamels above and normal prismatic enamels below in single mammalian species (data from Fosse 1968b; Fosse et al. 1978, 1985). Mean central distances between prisms in different taxa vary in normal prismatic as well as gigantoprismatic enamels. The variation within each type of enamel seems to describe its own statistical universe, however.

Recently some authors including myself have used the term "microprismatic" for ptilodontoid and most other mammalian enamels. This might imply that there is also a medium prism size. Therefore all non-taeniolabidoid (*sensu* Sloan and Van Valen 1965) enamels should be designated "normal".

Whether the different crystal aggregates (prisms?) shown in Fig. 5 have had a relation to original ameloblasts like normal prisms and continue into the enamel below the micrographed surface is questionable. A more superficial planed and etched enamel surface planoparallel to the one in Fig. 5 in the same tooth was also micrographed and showed a much higher relative number of the smaller crystal bodies (see Fosse et al. 1991). Thus there seems to be no point in calculating their numerical density since a corresponding variation in cell size (CD) within a population of enamel producing ameloblasts is improbable. Enamel etching lasted maximally 5 secs using 5% HNO₃ and was always interrupted by rinsing in pure water (Fosse 1968c; Fosse et al. 1985). Recrystallization after etching is therefore very improbable as no precipitation could oc-



Fig. 5. SEM micrograph of planed and etched I2 enamel of Plagiaulacinae gen. et sp. indet. DORCM GS 8, Purbeck Limestone Formation (from Fosse et al. 1991). There are numerous large round, barnacle-like structures varying in form and size, each seemingly consisting of crystals converging toward the outer enamel surface and surrounding an often slit-like opening from which a filamentous structure may protrude. Between them are much smaller circular crystal aggregates. Scale bar 10 μ m.

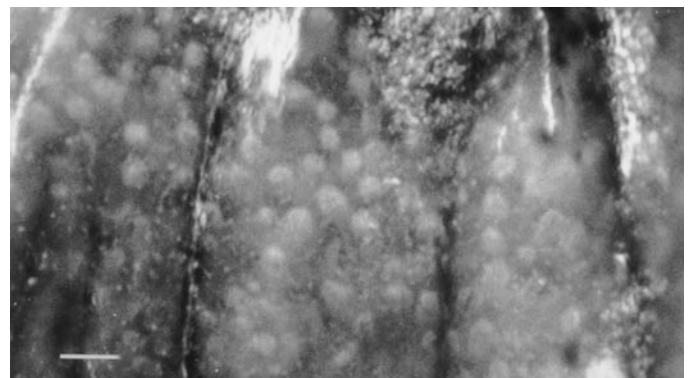


Fig. 6. Incident light micrograph of unplaned and unetched enamel of the plagiaulacid *Bolodon crassidens* MNH 47735, P1. Since the enamel mantle is strongly curved some of the natural surface is seen in the upper right quarter. Below, the focal plane is within the enamel and light is reflected from irregularly distributed circular bodies there. In irregular distribution between the larger bodies, much smaller spherical bodies may be discerned. If this enamel were planed and etched it might perhaps look like the plagiaulacidan enamel in Fig. 5. Scale bar 20 μ m.

cur and it is no more probable than for the derived cimodontan enamels. Clusters of bodies of the same size and distribution as the larger structures in Fig. 5 were also seen in unplaned and unetched enamels by incident light microscopy in this and other specimens of Purbeck multituberculates (Fig. 6). Furthermore, size and distribution of prisms are identical using SEM techniques with etching or with polarized light microscopy without etching (Fosse et al. 1973, 1985). Thus Jurassic plagiaulacidan enamels in plesiomorphic and geologically older multituberculates deserve a closer, more invasive examination regarding the continuity of possible structures from inner to outer enamel surface, to compare with more derived multituberculate enamel forms. Also an important aim is to describe micromorphological, evolutionary stages between the types represented in Figs. 3 and 5.

Acknowledgements.—I thank the journal reviewers Wighart von Koenigswald, Thomas Martin, and Craig B. Wood for their constructive criticism. I am also grateful to Richard L. Cifelli for correcting my English.

References

- Carlson, S.J. and Krause, D.W. 1985. Enamel ultrastructure of multituberculate mammals: an investigation of variability. *Contributions from the Museum of Paleontology, University of Michigan* 27: 1–50.
- Fosse, G. 1968a. The calculation of prism diameters and number of prisms per unit area in dental enamel. *Acta Odontologica Scandinavica* 26: 315–336.
- Fosse, G. 1968b. The numbers of cross-sectioned ameloblasts and prisms per unit area in tooth germs. *Acta Odontologica Scandinavica* 26: 573–603.
- Fosse, G. 1968c. Serial etching of dental enamel. *Acta Odontologica Scandinavica* 26: 285–297.
- Fosse, G., Risnes, S., and Holmbakken, N. 1973. Prisms and tubules in multituberculate enamel. *Calcified Tissue Research* 11: 133–150.
- Fosse, G., Eskildsen, R., Risnes, S., and Sloan, E. 1978. Prism size in tooth enamel of some Late Cretaceous mammals and its value in multituberculate taxonomy. *Zoologica Scripta* 7: 57–61.
- Fosse, G., Kielan-Jaworowska Z., and Skaale, S.G. 1985. The microstructure of tooth enamel in multituberculate mammals. *Palaeontology* 28: 435–449.
- Fosse, G., Kielan-Jaworowska, Z., and Ensom, P.C. 1991. Enamel ultrastructure of Late Jurassic multituberculate mammals. In: Z. Kielan-Jaworowska, N. Heintz, and H.A. Nakrem (eds.), Fifth Symposium on Mesozoic Terrestrial Ecosystems and Biota. Extended Abstracts. *Contribution from the Paleontological Museum, University of Oslo* 364: 25–26.
- Fosse, G., Rădulescu, C., and Samson, P.M. 2001. Enamel microstructure of the Late Cretaceous multituberculate mammal *Kogaionon*. *Acta Palaeontologica Polonica* 46: 437–440.
- Fox, R.C. 1999. The monophyly of the Taeniolabidoidea (Mammalia: Multituberculata). In: H.A. Leanza (ed.), *VII International Symposium on Mesozoic Terrestrial Ecosystems. Abstracts.*, p. 26. Buenos Aires.
- Kielan-Jaworowska, Z. and Hurum, J. 2001. Phylogeny and systematics of multituberculate mammals. *Palaeontology* 44: 389–429.
- Koenigswald, W., von and Sander, P.M. (eds.) 1997. *Tooth Enamel Microstructure*. 180 pp. Balkema Press, Rotterdam.
- Krause, W. D. and Carlson, S. J. 1986. The enamel ultrastructure of multituberculate mammals: a review. *Scanning Electron Microscopy, for 1986*: 1591–1607.
- Krause, W.D. and Carlson, S.J. 1987. Prismatic enamel in multituberculate mammals: tests of homology and polarity. *Journal of Mammalogy* 68: 755–765.
- McKenna, M.C. 1975. Toward a phylogenetic classification of the Mammalia. In: W.P. Luckett and F.S. Szalay (eds.), *Phylogeny of the Primates*, 21–46. Plenum Publishing Corporation, New York.
- Sloan, R.E. and Van Valen, L. 1965. Cretaceous mammals from Montana. *Science* 148: 220–227.

Gisle Fosse [gisle.fosse@nhm.uio.no], Geologisk Museum Boks 1172, Blindern 0318 Oslo, Norway.